



Published in final edited form as:

Anal Chem. 2010 March 15; 82(6): 2505–2511. doi:10.1021/ac9029345.

Fabrication of Two-Layered Channel System with Embedded Electrodes to Measure Resistance Across Epithelial and Endothelial Barriers

Nicholas J. Douville[†], Yi-Chung Tung[†], Ran Li[‡], Jack Dong Wang[†], Mohamed E.H. El-Sayed[†], and Shuichi Takayama^{†,§}

Shuichi Takayama: takayama@umich.edu

[†]Department of Biomedical Engineering, University of Michigan, Ann Arbor, MI 48109, USA

[‡]Department of Chemical Engineering, University of Michigan, Ann Arbor, MI 48109, USA

[§]Department of Macromolecular Science & Engineering, University of Michigan, Ann Arbor, MI 48109, USA

Abstract

This manuscript describes a straightforward fabrication process for embedding Ag/AgCl electrodes within a two-layer PDMS microfluidic chip where an upper and a lower channel are separated by a semi-porous membrane. This system allows for the reliable real-time measurement of trans-endothelial and trans-epithelial electrical resistance (TEER), an accepted quantification of cell monolayer integrity, across cells cultured on membranes inside the microchannels using impedance spectroscopy. The technique eliminates the need for costly or specialized microelectrode fabrication, enabling commercially available wire electrodes to easily be incorporated into PDMS microsystems for measuring TEER under microfluidic environments. The capability of measuring impedance across a confluent cell monolayer is confirmed using (i) brain-derived endothelial cells (bEND.3), (ii) Madin Darby Canine Kidney Cells (MDCK-2), and mouse myoblast (C2C12) (all from ATCC, Manassas, VA). TEER values as a function of cell type and cell culture time were measured and both agree with previously published values from macro-scale culture techniques. This system opens new opportunities for conveniently resolving both trans-endothelial and trans-epithelial electrical resistance to monitor cell function in real-time in microfluidic cell cultures.

Keywords

Trans-endothelial electrical resistance; Trans-epithelial electrical resistance; TEER; Blood Brain Barrier; bEND.3; Impedance Spectroscopy; Impedance Spectra; Barrier Integrity; Microfluidic Endothelium; Microfluidic Epithelium

Trans-membrane electrical resistance offers a quantitative technique to measure the integrity of the tight junctions that govern solute transport across the paracellular space of endothelial

SUPPORTING INFORMATION AVAILABLE:

Matlab Programs for resolving TEER from Impedance Spectra (circuit_fit.m and circuit_fun.m)

Representative Impedance Spectra for bEND.3 Cells over One Week Growth

Comparison of Impedance Spectra for Porous Polyester and PDMS membranes

The Impact of FN treatment on Impedance Spectra

Inherent Measurement Variance

Impact of Treatment with TritonX-100

and epithelial monolayers.¹ Because impedance values can be recorded in real-time without damaging cells, it is expected to be particularly useful for dynamic microfluidic experiments. Existing systems for measuring TEER, however, are limited to static or macroscopic cell environments and difficult to adapt to microchannels. The challenge arises because of: (1) the small cell culture area for TEER measurement, (2) the high electrical resistance along the length of the microchannel, dictating electrode placement in immediate proximity of the cell culture area, (3) and measurement-to-measurement variances if the recording electrodes are not secured within the channel. A convenient and robust channel design and fabrication procedure for embedding electrodes within poly(dimethylsiloxane) (PDMS) microsystem for the purpose of taking TEER measurements within microfluidic systems is presented. The system is characterized by measuring impedance across monolayers of three common cell lines (i) C2C12, (ii) bEND.3 (endothelial), and (iii) MDCK-2 (epithelial) over 7 days of static growth.

Technologically, measurement of electrical properties within microfluidic systems or other small scale systems has previously been reported for applications ranging from flow cytometry^{2,3,4} to patch clamping^{5,6,7} to electrophoresis^{8,9} to electrochemical detection¹⁰ however, these techniques require electrode deposition onto a rigid substrate such as silica which greatly limits the diffusion of oxygen and carbon dioxide required for cell culture.¹¹⁻¹² Embedding and immobilizing TEER recording electrodes directly within the microfluidic channel, in close proximity to the cell monolayer, eliminates the systemic electrical resistance of growth media within the microchannel and reduces signal noise resulting from electrode motion. Efforts to deposit recording electrodes (Au, Pt, and Ag) directly onto a PDMS substrate were limited by frequent cracking due to Modulus differences between conductive metals and elastomeric PDMS polymer and attempts to directly integrate macro-scale recording devices resulted in noise obscuring the signaling value (data not shown). Deposition-free integration of metallic electrodes into two-layered microfluidic channels;^{13,14} would enable upper and lower channels to be fabricated entirely from PDMS without the presence of a rigid silica substrate. This could potentially improve gas diffusion and allow co-culture of multiple cell types on opposing sides of a membrane.

Biomedically, microfluidic systems are emerging as useful platforms for modeling cellular barriers. This is because these systems offer precise control over physiologic stresses,^{15,16,17} chemical signaling,¹⁸ and the degree of cell-cell interaction.¹¹ One challenge has been the development of convenient and quantitative measures of the integrity of the cell barrier in microfluidic devices. Barrier integrity, specifically tight junctional control over the paracellular permeability of an endothelial or epithelial monolayer, can be characterized in vitro through quantitative techniques including (i) trans-endothelial/epithelial electrical resistance (TEER), (ii) measuring the permeability of radiolabeled paracellular permeability markers like mannitol; and qualitative tests including (i) freeze-fracture electron microscopy of trans-membrane fibrils, and (ii) immunostaining for proteins characteristic of tight junctions (occludin, ZO-1, and ZO-2). Because TEER offers quantitative monitoring of the monolayer integrity without damaging or altering the cell phenotype, it is expected to be particularly useful for time-lapse analysis of microfluidic experiments.

EXPERIMENTAL SECTION

Materials and Reagents

Poly(dimethylsiloxane) (PDMS) (Sylgard 184) was purchased from Dow Corning (Midland, MI). SU-8 2150 for two-step positive photoresist features was purchased from MicroChem Co. (Newton, MA). Polytester membranes were purchased from Corning Inc. (Corning, NY). All cell lines were purchased from ATCC (Manassas, VA). Ag/AgCl electrodes of 500 μm diameter were purchased from World Precision Instruments (Sarasota, FL).

Device Design and Fabrication

The device is composed of two layers of PDMS microfluidic channels, which are designed with integrated micro-grooves that permit the physical registration of two electrodes on opposite sides but in immediate proximity to a porous membrane on which cells are cultured for impedance measurement.¹⁹ The porous membrane on which cells attach and grow (initial diameter 24 mm and with a thickness of 10 μm) is first cut from the TransWell casing using a scalpel and trimmed to a size slightly larger than the area of overlap between the upper and lower channels (2 mm \times 2 mm). The cut membrane was then sandwiched between two PDMS channels. The elastomeric nature of the PDMS material combined with sealing of any crevices by PDMS mortar,¹³ allows sealing of the channel despite the 10 μm thickness of the membrane. Figure 1 provides an overview of the device design. The deposition-free integration of metallic electrodes alleviates the delaminating problem between metallic thin films and PDMS surfaces. Moreover, the fabrication process can be performed in the ambient environment without using sophisticated thin film deposition instruments in environment-controlled cleanrooms. Such microfluidic device design is capable of providing more functionalities and robust measurement results without increasing fabrication complexity.

The microfluidic channels on each PDMS layer were designed to have cross-sectional areas of 2000 μm (width) by 200 μm (height), and an additional channel groove (500 μm \times 500 μm) intersecting the main channel at a 45° angle for the measurement electrodes as shown in Figure 2. The fabrication of the PDMS chips was conducted using soft lithography technique. A silicon wafer with two-step positive relief features fabricated using negative tone photoresist (SU-8 2150, MicroChem Co., Newton, MA) patterned by two separate photolithography steps was used as a mold. The mold was then silanized with tridecafluoro-1,1,2,2-tetrahydrooctyl-1-trichloro-silane (United Chemical Technologies, Bristol, PA) in a dessicator for more than 30 minutes at room temperature to prevent unwanted bonding. PDMS (Sylgard 184, Dow Corning) pre-polymer mixed at a weight ratio of 12 (prepolymer):1 (curing agent) was poured on the mold and cured overnight. The cured PDMS layers were removed from the wafer and reservoir holes were punched within the upper PDMS layer allowing access to both the upper and lower channels (Figure 2). Ag/AgCl recording electrodes with a diameter of 500 μm (World Precision Instruments, Sarasota, FL) were fit into the 500 μm \times 500 μm side channel and held by elastomeric tension through the sealing process. The electrodes were loaded through the entire length of the side channel but did not completely enter the main channel so that the confluency of the cell monolayer could be easily imaged. A 24 mm diameter (10 μm thickness) semi-porous polyester membrane with pore size of 400 nm (Corning Inc., Corning, NY) was cut into square sheets slightly greater than the overlapping area between the upper and lower channels (2 mm \times 2mm) to completely cover the overlapping region. A PDMS mortar solution (3 Toluene:2 PDMS by weight) was spun onto a glass microscope slide at 500 rpm for 5 seconds followed by 1500 rpm for 60 seconds to spread the mortar evenly along the entire surface of the glass slide. The upper and lower slabs of PDMS were contact printed onto the glass slide contact spreading the PDMS-Toluene mortar onto the flat substrate while sparing the recessed channel features. The edges of the polyester membrane were also “stamped” onto the PDMS-Toluene Mortar before being placed over the overlapping region between the upper and lower slabs of PDMS to seal the channels.¹³ After sealing the layered channels, PDMS prepolymer at a weight of 3 (prepolymer):1 (curing) agent was injected into the side channel using an 18 gauge blunt syringe needle. PDMS flow from the syringe was limited only to the side channel and flow was stopped before the PDMS prepolymer could flow into the main “cell culture” channels or immerse the tip of the electrodes. Flow was discontinued by holding pressure constant within the loading syringe containing PDMS pre-polymer (sealed via elastomeric tension with the inlet reservoir punched into the PDMS). To further restrict PDMS flow into the main channels, the chip was elevated so that the main channel (and electrode tip) remained

at a higher point than the side channel. The PDMS was allowed to cure for 24 hours at room temperature and the process was repeated for the second electrode.

Cell Seeding and Culture

Epithelial (MDCK-2) and endothelial (bEND.3) cell lines were selected because they offered well-characterized and accepted TEER values to compare the experimental results. Since mouse myoblast cells (C2C12) are not expected to form tight junctions, they were selected as a control cell-line to demonstrate measurement variability inherent to the system or any impedance drift resulting from prolonged cell culture. All cell lines were cultured in endothelial growth media (DMEM with 10% fetal bovine serum and 1% penicillin/streptomycin) prior to seeding in the microfluidic chip. The microfluidic chip was exposed to plasma oxygen for 5 minutes to make hydrophilic. Prior to cell seeding, fibronectin solution (Invitrogen) at a concentration of 100 $\mu\text{g/mL}$ in PBS was injected into the upper (endothelial) channel to promote cell adhesion. The lower channel was pre-loaded with growth media. Since the fibronectin solution adheres to the porous membrane as well as the surrounding PDMS microchannel walls, cells have the potential to adhere and divide along the channel walls; however, due to the orientation and geometry of the system and gravity-driven pumping mechanism, the vast majority of cells adhere directly to the porous membrane. The fibronectin solution remained in the upper channel for 30 min at 25°C under ultraviolet light to sterilize the system. After UV sterilization, sterile techniques and conditions were maintained. Following 30 minutes of fibronectin coating, the channel was completely washed with growth media to remove the non-adsorbed fibronectin and filled with growth media until seeding. Cells were trypsinized, centrifuged, and re-suspended in 1 mL of growth media (to a concentration $\sim 10^5$ cells/mL). The cell suspension was then flowed through the upper channel until pressure gradient between the inlet and outlet equilibrated eliminating flow. The cells were allowed to adhere under this static condition (no flow) for ~ 12 hrs before fresh media was flowed through the channel. The growth media was completely replaced with fresh media approximately every 12 hrs for the duration of the experiment. Immediately after seeding and for the duration of the culture time, the entire microfluidic system was kept in an incubation chamber (37°C, 5% CO₂). After successful cell seeding, cells rapidly divided until confluence. After reaching confluence, cells were successfully maintained within the microfluidic system for over 7 days of experimental measurement.

Impedance Spectroscopy

Impedance Spectra were taken using an Autolab potentiostat/galvanostat (EcoChemie). Alternating current of amplitude 0.1 V was passed between the two embedded Ag/AgCl electrodes in the frequency range from 10 Hz to 1.00 MHz, yielding a total of 64 impedance measurements (8 per decade spaced logarithmically). The total time for a single frequency scan was approximately 7 minutes.

Resolving TEER from Circuit Model

In order to resolve the TEER value from the experimental impedance spectra, the control impedance spectra (taken from the same chip just before cell seeding) was subtracted from the measured impedance spectra (with cells) to eliminate the affect from electrolyte, membrane and electrode-electrolyte interfaces and simplify the analysis. An equivalent lumped element circuit model (as shown in Figure 1) was used to simulate the cell monolayer electrical behavior. The circuit is constructed by three components, where R_E , R_I , and C_M represent extracellular (TEER), intracellular resistances and a membrane capacitance, respectively.^{20-21, 22} In order to resolve the value of each component, a MATLAB (The MathWorks, Inc., Natick, MA) code using its optimization tool box to estimate the values (Supporting Information) was developed. In the MATLAB code, the objective minimized the absolute

difference between the simulated and experimental impedance values under various frequencies. The TEER value determined by the MATLAB algorithm was then normalized for surface area of the cell monolayer (specifically 0.04 cm^2) by multiplying the total impedance yielding reported values in units of $\Omega \cdot \text{cm}^2$.

RESULTS AND DISCUSSION

Characterization of System

Prior to seeding cells, the baseline impedance of the system (electrodes, electrolyte, and polyester membrane) was characterized. In initial experiments, the electrolyte solution contained within the microchannel as well as switched from a low-impedance polyester membrane to a high-impedance PDMS membrane was varied. Increasing the concentration of the KCl electrolyte from 0.1 M to 1.0 M resulted in a frequency-independent impedance decrease of greater than $1.5 \text{ k}\Omega$ (Figure 3a). Replacing the porous polyester membrane with a PDMS membrane of similar thickness but without pores ($\sim 10 \text{ }\mu\text{m}$) increased the impedance of the system from $100 \text{ k}\Omega$ (polyester) to $\text{M}\Omega$ (PDMS) range. The PDMS membrane also contributed a capacitive effect to the impedance spectra (Supplementary Information Figure 4). These experiments verified that the system correctly detected expected impedance changes. The impact of FN-treatment on the baseline impedance of the system was also tested. Baseline system impedance was recorded for 3 chips filled with PBS. Next fibronectin in PBS (at a concentration of $100 \text{ }\mu\text{g/mL}$) was loaded into the system, allowing the fibronectin to deposit for 30 minutes, before the channel was flushed with fresh PBS. These results showed that FN-treatment had a minimal impact on the impedance of the system (Supplementary Information Figure 5). The impedance of a channel filled with endothelial growth media (DMEM), Phosphate Buffered Saline (PBS), and 0.1 M KCl (no fibronectin was added to the system during these comparison controls) was also measured. The impedance of the system containing 0.1 M KCl had the lowest impedance, the PBS had intermediate impedance, and the growth media had the highest impedance (Figure 3b). This experiment demonstrated the feasibility of recording through channels containing endothelial growth media; eliminating the need for a specifically conductive electrolyte solution for cell recordings.

Traditional recording systems record impedance values at either DC current or a limited number of a AC frequencies.^{23,24,25} Measuring at high frequency minimizes, but does not completely eliminate impedance resulting from the capacitive cell membrane. While sufficient for taking TEER measurements across a large area such as in TransWell cultures particularly when the TEER values are large, measuring impedance across the full spectrum of AC frequencies enables the characteristic of the cell monolayer to be more accurately modeled and resolved.^{26,27,28,29} The smaller microfluidic system is inherently prone to lower signal to noise ratios. For example, the surface area of the system is 0.04 cm^2 compared to a surface area of 4.91 cm^2 in the 6-well TransWell Culture systems most commonly used for TEER measurements (and 0.143 cm^2 even in 96-well TransWell Cultures which are considered very small). Thus, in addition to placing and immobilizing electrodes close to the cells, we measure impedance at over 64 frequency points and use this data to find the best fit to the entire equivalent circuit (Figure 1.) and resolve out factors that can vary independently of TEER.

A relatively large variability in impedance between different chips was found, most likely due to variance in the distance between the two electrodes caused by alignment variations of the upper and lower channel. It is estimated that for every mm difference in the distance between the two recording electrodes, the resistance changes by approximately $2.5 \text{ k}\Omega$.³⁰ Variability between different measurements within a single chip (where the electrodes remain fixed), however, was minimal. Thus, in the experimental TEER measurements, the baseline impedance of each individual chip was characterized prior to endothelial cell seeding and

subtracted from the impedance of the cell monolayer within the chip. This allowed a circuit model to be fit that accounted for contribution of the cell monolayer.

Establishing a Baseline Measure

As an experimental control and to establish a baseline measure, we measured the impedance of the system for one week under two conditions: (i) without cells (acellular) and (ii) with cells not expected to form tight junctions (C2C12 cell culture). In both conditions the media was replaced with fresh media twice per day. Although no cells were cultured in the first control, TEER values were fit using the MATLAB algorithm and the experimental data was normalized to total membrane surface area. The data are summarized in the Supplementary Information. Measurements of the system containing growth media without cells (Supplementary Information, Figure 6) showed relatively minimal change in TEER [$<10 \Omega \cdot \text{cm}^2$ in either the positive or negative direction] when compared to the magnitude of TEER changes which result from tight junction formation in endothelial and epithelial cell lines [$\sim 100 \Omega \cdot \text{cm}^2$ in the positive direction]. Furthermore, the absence of either a positive trending TEER (as expected from protein deposition on the electrodes) or negative trending TEER (as expected if the Ag/AgCl electrodes were being re-conditioned during testing) through 7 days of measurements (the first day is the baseline) indicate that the system is stable for long-term experimental measurements in serum-containing media. Because the TEER fluctuations do not trend in either the positive or negative direction, we hypothesize that these changes indicate the baseline level of noise or error in the system resulting from recording equipment as well as other variables that could not be perfectly controlled such as temperature fluctuation in the incubator, precise attachment of system to recording equipment, or resistivity of the DMEM solution. Next, changes in TEER resulting from culturing a cell line not expected to form tight junction, were measured. The electrical resistance across a C2C12 monolayer (Figure 4c) displayed a minimal increase [$<20 \Omega \cdot \text{cm}^2$ in the positive direction] indicating that the physical presence of cells or cellular by-products results in a non-trivial increase in monolayer resistance despite the theoretical absence of tight junctions which is able to be resolved from TEER changes resulting from tight junction formation.

TEER as a Function of Time with Epithelial and Endothelial Cells

MDCK-2 and bEND.3 cells were seeded onto the fibronectin-treated membrane. Impedance spectra were taken each day for 7 consecutive days. Because temperature influences the impedance of the growth media, measurements were consistently taken 30 minutes after fresh media was loaded into the system and the system was kept incubated at 37 °C before and between all measurements. TEER values were resolved from the Impedance Spectra taken on each day following seeding using a best-fit circuit algorithm (Supporting Information). Data showed that TEER values increased with each day of growth from Day 1 to Day 3–4 before reaching a plateau and even decreasing slightly. The error bars depicted in Figure 4 a,b,c is the standard deviation of the 9 TEER values that can be resolved on each day, for each cell type. The experimental data agreed with the accepted TEER range of 150–200 $\Omega \cdot \text{cm}^2$ for bEND.3 cells³¹ and 50–150 $\Omega \cdot \text{cm}^2$ for MDCK-2 cells.³² Additionally, both cell lines followed an increase-plateau-decrease pattern similar to previously published models and significant differences between each of the three chosen cell lines could be resolved (Figure 4).

Dynamic Impedance Changes in Response to Chemical/Protein Treatment

To demonstrate that our system can detect dynamic impedance changes in response to chemical factors, the impedance of a bEND.3 cell monolayer was measured, then the cell monolayer was treated for 30 minutes with TritonX-100 (0.1% in DMEM),³³ before the system was flushed with fresh DMEM and the impedance was re-measured. Our experimental results showed that the impedance of the entire system decreased significantly at all frequency points

following treatment with TritonX-100 (Supporting Information, Figure 7a). The change in TEER (paracellular resistance) was also resolved using the MATLAB circuit fitting algorithm, and found decrease from $161.51 \pm 0.755 \Omega \cdot \text{cm}^2$ to $39.73 \pm 1.925 \Omega \cdot \text{cm}^2$ (Supporting Information, Figure 7b).

Furthermore, a change in the impedance at all frequency points following trypsinization was demonstrated (Supporting Information, Figure 3). The decrease in impedance amplitude shows that the system and technique are capable of detecting changes in response to chemical or protein treatment in real-time.

The Potential Impact of Fluid Flow—All of the experimental data were taken in the static case (absence of fluid flow). Readings taken during fluid flow may impact TEER measurements but we envision that the flow can always be stopped during short durations of measurements.

Comparison to Existing TEER Measurement Systems

To enable reliable TEER measurement across the small cell culture area within microfluidic channels, the system incorporates features adapted from multiple advances that have been made over the years for macroscopic TEER measurement systems.³⁴ The most widely used system for measuring TEER *in vitro* is the commercially available TransWell culture environment and the “chopstick-style” recording electrode.^{35,36} For more reproducible and stable TEER measures of leaky cell barriers with lower TEER values, improved recording chambers with embedded electrodes have been constructed. An example is the Endohm chamber, where electrodes are placed immediately above and beneath the membrane to minimize resistance from the media and allow a more uniform current density to flow across the membrane. The microfluidic chamber incorporates a similar concept by embedding electrodes immediately above and below the cell culture membrane inside the channels. Another enhancement in measurement is represented by the cellZscope²⁸ which can measure the impedance across a wide spectrum of frequencies, rather than the typical one frequency, to give more detailed measures of barrier properties. The microfluidic TEER measurement system also acquires impedance spectra at 64 frequencies to obtain more accurate TEER values.³⁷ Giaever and colleagues developed an alternative system that does not use porous membranes to measure endothelial barrier function of cells directly grown on gold electrodes.²⁴ This system has the advantage of enabling measurements of cell barrier functions over very small areas. We initially attempted to mimic this system by forming gold electrodes inside PDMS microchannels, but found that the flexibility of PDMS led to cracking of gold, limited the conductivity.³⁸ The membrane embedded microfluidic TEER system we describe, however, still enables measurements to be made over relatively small cell culture areas. Additionally, by keeping the membrane sandwiched multilayer channel structure, our system enables basal cell treatment that is critical for optimal signaling in some cellular systems.³⁹ Perhaps the most related device setup is that reported by Harris and Shuler where TEER was measured across a small area of cells cultured on a thin silicon nitride membrane with a custom electrode-embedded chamber.⁴⁰ The reported TEER values from this device, however, were very low due to cell culture problems making it difficult to validate functionality or make comparisons. Hediger and colleagues have also developed microfabricated systems for characterizing epithelial cell tissues.^{41, 42} In their system, a nano-porous polycarbonate membrane is glued between two microscale reservoirs. Their design allows trans-epithelial resistance to be measured in a glass or PDMS microsystem; however, was limited by multiple fabrication steps and a multi-layered modular arrangement. Further advances in microfluidically analyzing the electrical properties of cells are reviewed by Bao, Wang, and Lu.⁴³

Comparison to Existing Techniques for taking Electrical Recordings with Microfluidic Systems

There have been several reported methods for integrating electrodes within microfluidic systems.^{44,45,46} In a method developed by Garcia and Henry, a gold wire was aligned within a perpendicular microfluidic channel and sealed using super-glue and conducting paint.^{47,48} Electroplating and electroless deposition have been used to fabricate recording electrodes within microfluidic systems but are limited by multiple slow and costly lithographic steps and the requirement for a smooth rigid substrate.⁴⁹ Die, impression, and injection molding, have also proven useful for very specialized approaches but are limited by the high cost and complexity of the system.⁵⁰ The systems described in this manuscript can be easily fabricated using standard soft-lithography techniques and utilize readily available and standardized electrodes which should enable this technique to be easily expanded to other models and systems.

The procedure described in this paper combines recent advances from a variety of scientific disciplines including cell biology (impedance spectroscopy), microfluidic fabrication, and electrical engineering (flexible electronic circuits) to create cell culture microenvironments with real-time, non-damaging read outs of cell functions. The procedure described in this paper has six advantages to existing fabrication techniques, which makes it especially useful and versatile: (i) all steps are based in traditional soft-lithography procedures and do not require unique metal deposition components; (ii) the electrodes utilized are inexpensive, well-characterized, and commercially available; (iii) the cell culture membrane is taken directly from TransWell culture wells, the membrane most commonly used in TEER systems; (iv) the recording electrodes are close to the permeable membrane and positioned appropriately to reliably measure TEER in real-time, from cells cultured over a small surface area without disrupting the integrity of cell membrane; (v) the fitting algorithm utilizing a full impedance spectra provides a more accurate representation of the TEER than traditional DC measurement or single frequency impedance measurement systems; (vi) the entire system is fabricated from PDMS polymer (no glass substrate) allowing gas exchange convenient for long term cultures.

The system design can continue to be improved by standardizing the fabrication protocol which will eliminate the chip-to-chip variance currently seen. The inclusion of an additional reference electrode could also potentially eliminate the system variance characterized in the Supplementary Information. The size of the electrode, relative to channel dimensions can also continue to be reduced.

CONCLUSION

A convenient channel design and fabrication procedure for measuring endothelial and epithelial cell barrier function within a PDMS microfluidic system is presented. This method for embedding Ag/AgCl recording electrodes within a side microfluidic channel can be easily replicated by any lab with soft-lithography capabilities utilizing widely available, well-characterized, and commercially available electrodes and membranes. Because our system is comprised of an upper and lower channel fabricated entirely from PDMS polymer, many of the limitations of existing microfluidic electrical recording systems, specifically the need for rigid, non-permeable substrate or costly and slow fabrication protocol can be avoided. Our fabrication method enables placement and immobilization of recording electrodes in close proximity to cells growing on a polyester membrane. Additionally, by combining this fabrication technique with circuit fitting using impedance spectroscopy, TEER values can be resolved from microfluidic cell culture platforms with much smaller surface areas compared to conventional culture systems. The biological utility of the electrode-embedded microfluidic system by non-invasively resolving endothelial and epithelial barrier function in for one week of cell culture is demonstrated. Our TEER results agreed with expected results in both value

and profile (increase—plateau). This system is expected to provide a valuable, real-time, quantitative measure of the effects of microfluidic cultures on cells under unique physiological two-layer microfluidic environments such as exposure to laminar flow and air-liquid two-phase flows, combined with basal signaling and basal side co-cultures.^{16,17}

Supplementary Material

Refer to Web version on PubMed Central for supplementary material.

Acknowledgments

This work was supported by NIH (HL084370 and CA136829). N.J.D acknowledges financial support from the University of Michigan Medical Scientist Training Program (NIGMS T32 GM07863) and National Heart, Lung, And Blood Institute (F30HL095333). We thank Daryl Kipke, John Seymour, and Kip Ludwig of the Neural Engineering Laboratory (NEL) for use of the Autolab potentiostat/galvanostat and assistance with impedance spectra measurements and analysis. We thank Richard Keep, Paul Christensen, and Jon Song for their helpful discussions.

REFERENCES

1. Reichel, A.; Begley, DJ.; Abbott, NJ. An Overview of In Vitro Techniques for Blood-Brain Barrier Studies. In: Nag, S., editor. *The Blood-Brain Barrier: Biology and Research Protocols (Methods in Molecular Medicine)*. Vol. 89. Springer Protocols; 2003. p. 307-324.
2. Cheung K, Gawad S, Renaud P. *Cytometry Part A* 2005;65A:124–132.
3. Yao B, Luo G-A, Feng X, Wang W, Chen L-X, Wang Y-M. *Lab Chip* 2004;4:603–607. [PubMed: 15570372]
4. Simonnet C, Groisman A. *Anal.Chem* 2006;78:5653–5663. [PubMed: 16906708]
5. Pantoja R, Nagarath JM, Starace DM, Melosh NA, Blunck R, Bezanilla F, Heath JR. *Biosens. Bioelectron* 2004;20:509. [PubMed: 15494233]
6. Farinas J, Chow AW, Wada HG. *Anal. Biochem* 2001;295:138–142. [PubMed: 11488614]
7. Sinclair J, Olofsson J, Pihl J, Orwar O. *Anal. Chem* 2003;75:6718–6722. [PubMed: 16465721]
8. Sia SK, Whitesides GM. *Electrophoresis* 2003;24:3563–3576. [PubMed: 14613181]
9. Lagally ET, Simpson PC, Mathies RA. *Sens. Actuators, B* 2000;63:138–146.
10. Pai RS, Walsh KM, Crain MM, Roussel TJ, Jackson DJ, Baldwin RP, Keynton RS, Naber JF. *Anal Chem* 2009;81:4762–4769. [PubMed: 19459620]
11. Ayliffe HE, Frazier AB, Rabbit RD. *J.MEMS* 1999;8:50–57.
12. Iliescu C, Poenar DP, Carp M, Loe FC. *Sens. Actuators, B* 2007;123:168–176.
13. Chueh B-H, Huh D, Kyrtos CR, Houssin T, Futai N, Takayama S. *Anal. Chem* 2007;79:3504–3508. [PubMed: 17388566]
14. Wu H, Huang B, Zare RN. *Lab Chip* 2005;5:1393–1398. [PubMed: 16286971]
15. Walker GM, Zeringue HC, Beebe DJ. *Lab.Chip* 2004;4:91–97. [PubMed: 15052346]
16. Song JW, Gu W, Futai N, Warner KA, Nor JE, Takayama S. *Anal. Chem* 2005;77:3993–3999. [PubMed: 15987102]
17. Huh D, Fujioka H, Tung Y-C, Futai N, Paine R, Grothberg JB, Takayama S. *Proc. Nat. Acad. Sci* 2007;104:18886–18891. [PubMed: 18006663]
18. Atencia J, Beebe DJ. *Nature* 2005;437:648–655. [PubMed: 16193039]
19. Tung Y-C, Zhang M, Lin C-T, Kurabayashi K, Skerlos SJ. *Sens. Actuators, B* 2004;98:356–367.
20. Kuni, H.; Kinouchi, Y. *Proceedings of the 20th Annual International Conference of the IEEE EMBS*; 1998. p. 3108-3111.
21. Kim K-J, Borok Z, Ehrhardt C, Willis BC, Lehr C-M, Crandall ED. *J. Appl. Physiol* 2004;10:1152–1180.
22. Lewis SA, Wills NK. *J. Membrane Biol* 1982;67:45–53. [PubMed: 6178830]
23. Cerejido M, Robbins ES, Dolan WJ, Rotunno CA, Sabatini DD. *J.Cell Biol* 1978;77:853–880. [PubMed: 567227]

24. Giaever I, Keese CR. *Proc. Nat.Acad.Sci.USA* 1984;81:3761–3764. [PubMed: 6587391]
25. Stamatovic SM, Keep RF, Wang MW, Jankovic I, Andjelkovic AV. *J. Biol. Chem* 2009;284:19053–19066. [PubMed: 19423710]
26. Kottra G, Fromter E. *Pflugers Arch* 1984;402:409–420. [PubMed: 6522248]
27. Erben M, Decker S, Franke H, Galla H-J. *J. Biochem. Biophys. Methods* 1995;30:227–238. [PubMed: 8621882]
28. cellZscope – How It Works. NanoAnalytics.
29. Wegener J, Sieber M, Galla H-J. *J.Biochem.Biophys.Methods* 1996;32:151–170. [PubMed: 8844323]
30. Lee WG, Bang H, Yun H, Kim JA, Cho K, Chung C, Chang JK, Han D-C. *Current Applied Physics* 2008;8:696–699.
31. Koto T, Takubo K, Ishida S, Shinoda H, Inoue M, Tsubota K, Okada Y, Ikeda E. *Am. J. Path* 2007;170:1389–1397. [PubMed: 17392177]
32. Richardson JC, Scalera V, Simmons NL. *Biochim.Biophys.Acta* 1981;673:26–36. [PubMed: 6110442]
33. van de Ven AL, Adler-Storthz K, Richards-Kortum R. *J. Biomed. Opt* 2009;14(2):011012-1–011012-10.
34. Deli MA, Abraham CS, Kataoka Y, Niwa M. *Cell. Mol. Neurobiol* 2005;25(1):59–127. [PubMed: 15962509]
35. Mishler DR, Kraut JA, Nagami GT. *Am. J. Physiol.Renal.Physiol* 1990;258(6):F1561–F1568.
36. Hurst RD, Fritz IB. *J. Cell. Physiol* 1996;167:81–88. [PubMed: 8698844]
37. Seebach J, Dieterich P, Luo F, Schillers H, Vestweber D, Oberleithner H, Galla H-J, Schnittler H-J. *Lab. Invest* 2000;80(12):1819–1831. [PubMed: 11140695]
38. Tiruppathi C, Malik AB, Del Vecchio PJ, Keese CR, Giaever I. *Proc.Nat.Acad.Sci.USA* 1992;89:7919–7923. [PubMed: 1518814]
39. Song JW, Cavnar SP, Walker AC, Luker KE, Gupta M, Tung Y-C, Luker GD, Takayama S. *PLoS ONE* 2009;4(6):e5756–e5756. [PubMed: 19484126]
40. Harris, SG.; Shuler, ML. *Proceedings of the IEEE 2th Annual Northeast Bioengineering Conference*; 2002. p. 1-2.
41. Hediger S, Sayah A, Horisberger JD, Gijs MAM. *Sens. Actuators B* 2000;63:63–73.
42. Hediger S, Sayah A, Horisberger JD, Gijs MAM. *Biosens. Bioelectron* 2001;16:689–694. [PubMed: 11679245]
43. Bao N, Wang J, Lu C. *Anal. Bioanal. Chem* 2008;391:933–942. [PubMed: 18335214]
44. Siegel AC, Bruzewicz DA, Weibel DB, Whitesides GM. *Adv. Mater* 2007;19:727–733.
45. Gray DS, Tien J, Chen CS. *Adv.Mater* 2004;16:393–401.
46. Lacour P, Tsay C, Wagner S. *IEEE Electron Device Letters* 2004;25:792–794.
47. Garcia CD, Henry CS. *Anal. Chem* 2003;75:4778–4783. [PubMed: 14674454]
48. Garcia CD, Henry CS. *Analyst* 2004;129:579–584. [PubMed: 15213822]
49. Polk BJ, Stelzenmuller A, Mijares G, MacCrehan W, Gaitan M. *Sens. Actuators, B* 2006;114:239–247.
50. Martin RS, Gawron AJ, Lunte SM. *Anal. Chem* 2000;72:3196–3202. [PubMed: 10939387]

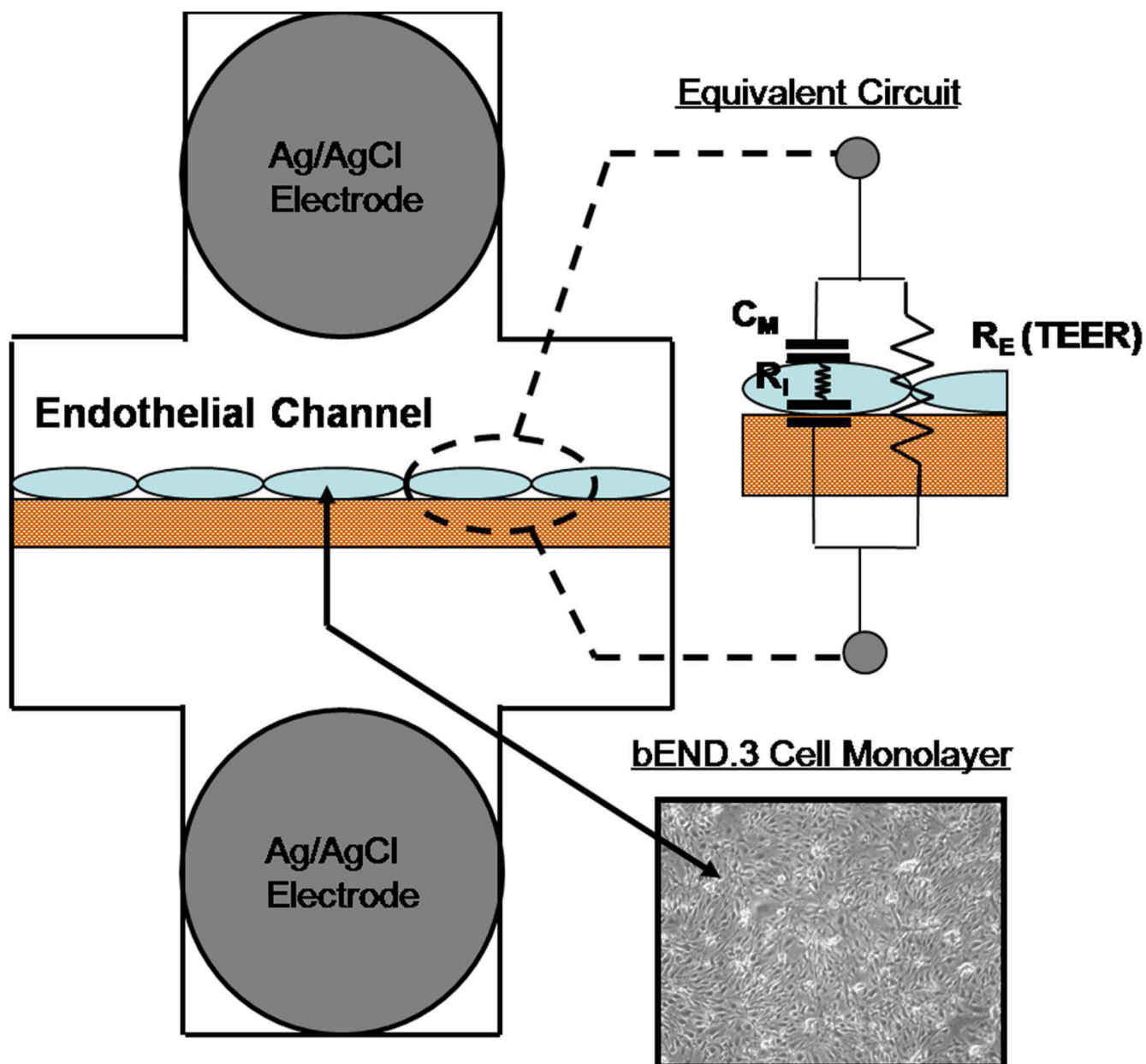


Figure 1. System Design with Equivalent Circuit Model

Ag/AgCl recording electrodes were embedded on opposing sides bEND.3 cells cultured on a polyester porous membrane. Electrical current has two parallel paths through a confluent cell monolayer. The transcellular path can be modeled by the internal resistance of a cell (R_I) in series with the capacitance of the cell membranes (C_M). The paracellular path is modeled by the resistor R_E and represents the trans-endothelial electrical resistance (TEER) of the experiment.

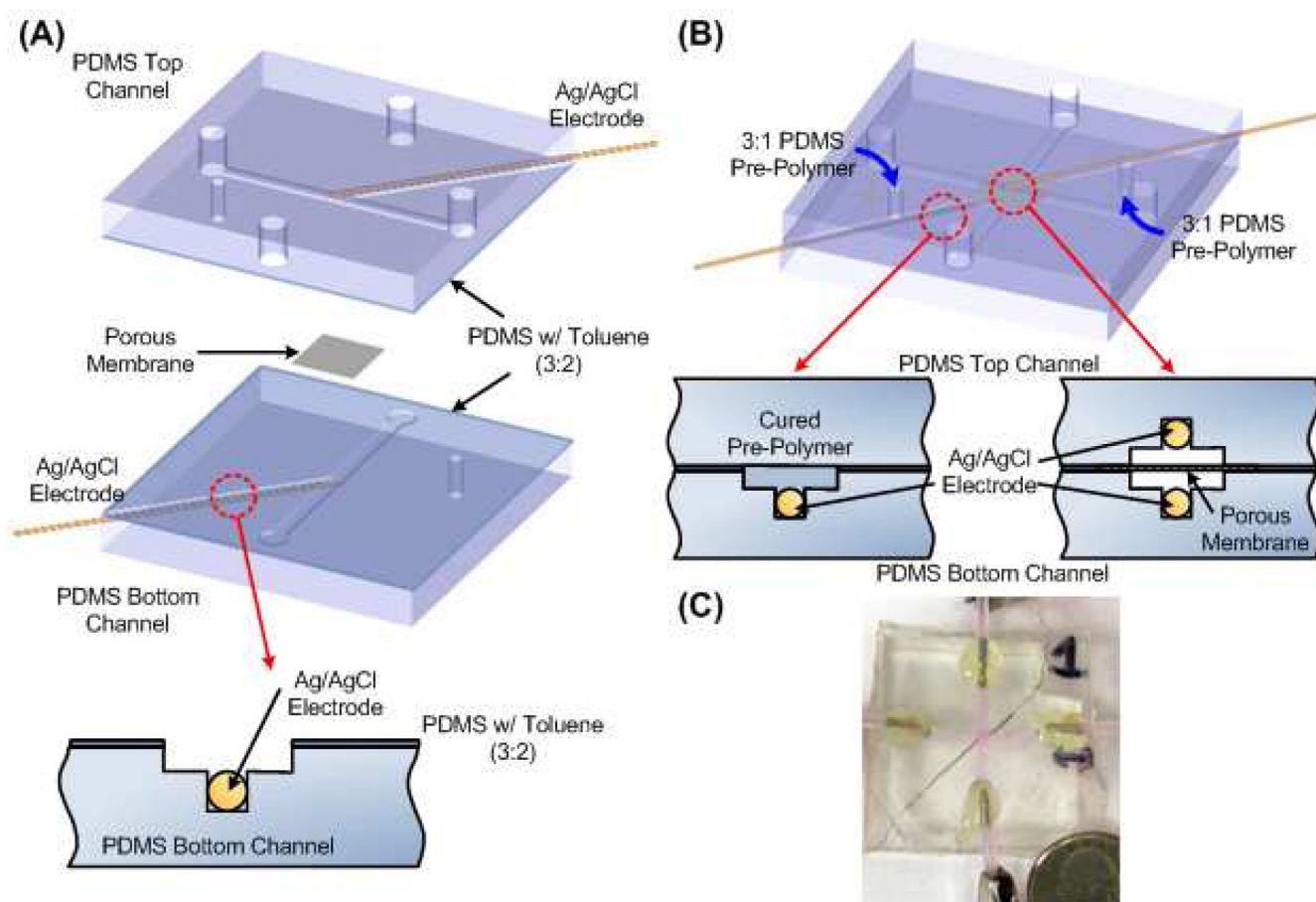


Figure 2. Fabrication Overview

(a) Device Bonding. Ag/AgCl wire electrodes were set into grooves of the same diameter fabricated within side channels. Upper and lower slabs were bonded using PDMS: Toluene stamping procedure. Chip was cured overnight at 60°C tightly bonding upper and lower slabs. (b) Securing Embedded Electrodes. 3 (PDMS prepolymer) : 1 (PDMS curing agent) was injected into the side channels. Flow was discontinued before PDMS prepolymer immersed the tip of the electrode or entered the main channel. Chip was elevated slightly during curing to prevent liquid polymer from draining into the main channel. Steps were repeated for the opposite electrode (orientation of the elevation was also switched). (c) Photograph of fabricated device.

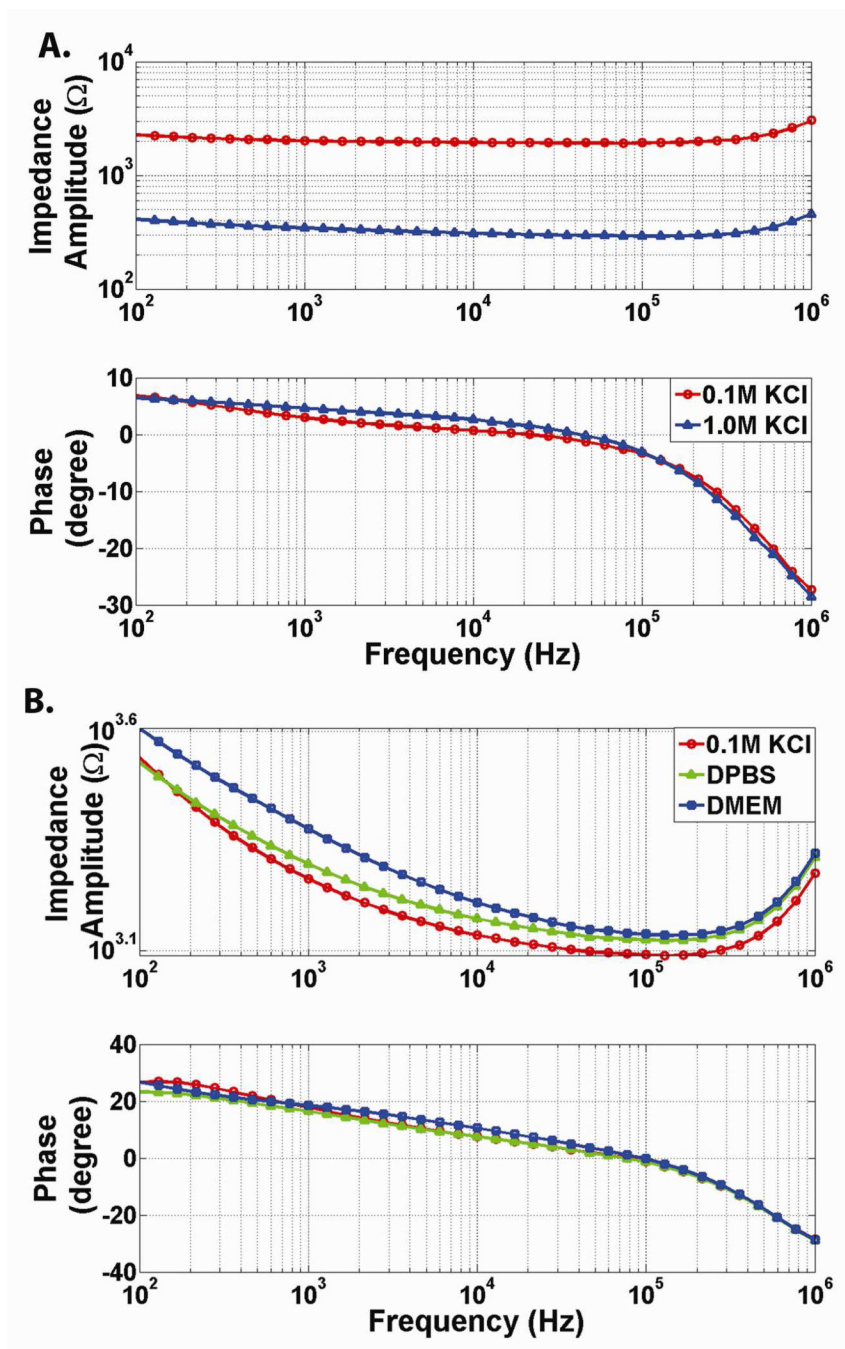


Figure 3. System Characterization

(a) Impact of Varying KCl Concentration on Impedance Spectra. As the concentration of KCl is increased from 0.1M to 1.0M, the resistivity of the electrolyte solution decreases leading to decreased resistance. Change in the concentration of KCl is expected to yield a purely resistive change (no impact on capacitance of the system). The frequency-independent impedance change confirms this expected result. (b) Impact of Varying Electrolyte Solution on Impedance Spectra. 0.1 M KCl has the lowest impedance. Phosphate Buffered Saline has intermediate impedance. Endothelial growth media has the highest impedance. Endothelial Growth Media (DMEM) is suitable for electrical recordings.

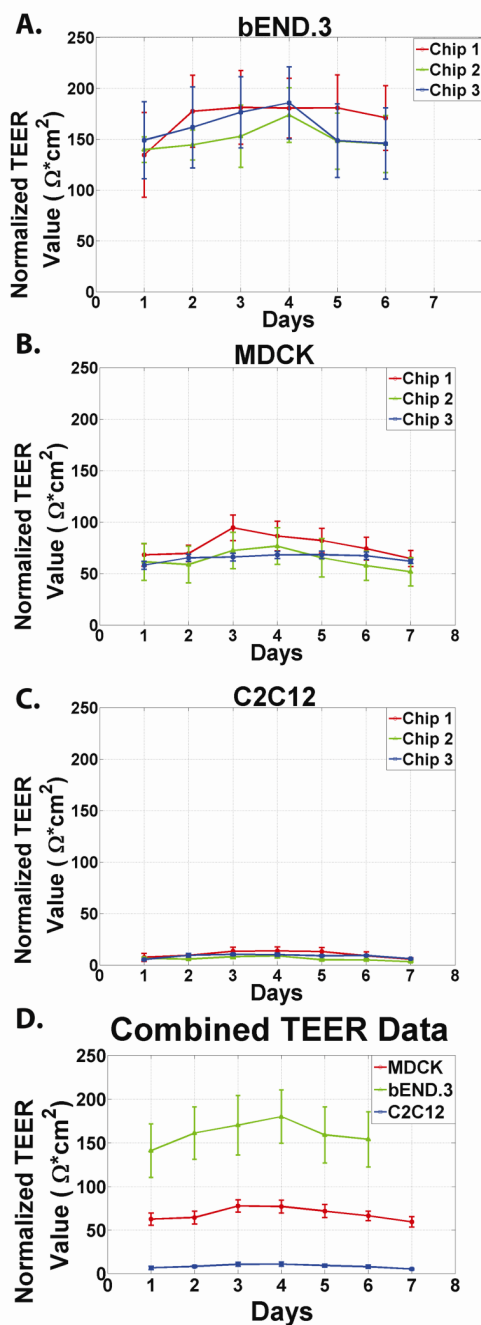


Figure 4. Resolved TEER as a function of days since Confluence for different cell lines

We seeded endothelial (bEND.3) and epithelial (MDCK-2) cell lines with well characterized barrier properties into our microfluidic system. For all cell lines, TEER increases for approximately 3–4 days following seeding before plateauing and decreasing slightly. Our data agreed with the accepted TEER range of 150–200 $\Omega \cdot \text{cm}^2$ for bEND.3 cells⁴⁸ and 50–150 $\Omega \cdot \text{cm}^2$ for MDCK-2 cells. Additionally, both cell lines followed an increase-plateau-decrease pattern similar to previously published models and significant differences between each of the three chosen cell lines could be resolved (Figure 4a, Figure 4b). Changes in TEER resulting from culturing a cell line not expected to form tight junction, were also measured. The electrical resistance across a C2C12 monolayer (Figure 4c) displayed a minimal increase [$<20 \Omega \cdot \text{cm}^2$

in the positive direction] indicating that the physical presence of cells or cellular by-products results in a non-trivial increase in monolayer resistance despite the theoretical absence of tight junctions. The data from the individual chips are combined in Figure 4d. Error bars represent standard deviations.